Journal of Electroceramics, 11, 227–239, 2003

Evaluation of Mixing Rules for Dielectric Constants of Composite Dielectrics by MC-FEM Calculation on 3D Cubic Lattice

YUGONG WU,* XUANHE ZHAO, FEI LI & ZHIGANG FAN

School of Electronic and Information Engineering, Tianjin University, Tianjin 300072, People's Republic of China

Submitted March 31, 2003; Revised July 15, 2003; Accepted January 9, 2004

Abstract. Effective dielectric constants of diphase composite dielectrics are simulated by Monte Carlo-finite element method on three-dimensional lattice. Effective dielectric constants with coefficients of variation less than 5.5% are obtained for different ratios of dielectric constants of the two phases, ranging from 10 to 700. Various mixing rules and equations are fitted to these data and the accuracy and relevance of the fits are thoroughly examined. Modified logarithmic rule loses its physical basis when fitted to three-dimensional data. As the ratio of dielectric constants of the two phases increases, the parameters in general Lichterecker mixing rule, general Bruggeman's symmetric equation, general effective media equation and its modified form all increase or decrease monotonously. General effective media equation and its modified form give the best fits to the effective dielectric constants simulated. The simulation results for the dielectric constants of some composite systems are in good agreement with experimental data.

Keywords: effective dielectric constant, Monte Carlo-finite element method, mixing rule

1. Introduction

Practical dielectric ceramics is commonly diphase or even multiphase composite. The presence of a second phase is sometimes mainly due to processing technique and may have a negative effect on the performance of that material. For example, in the preparation of Pb-based perovskite relaxor ferroelectrics (such as lead magnesium niobate, PMN), it is very difficult to fabricate pure perovskite phase without the formation of a pyrochlore phase, which obviously degrades performance of the materials [1, 2]. On the other hand, some phases are sometimes introduced purposefully, so that dielectric ceramics can satisfy special requirements such as specified dielectric constant and its temperature coefficient. For example, one can utilize phases with positive and negative temperature coefficients to compose dielectric material whose temperature coefficient is approximately zero by adjusting the volume fraction of each phase [3]. In both circumstances, it is highly desirable for an equation, or mixing rule, which can provide accurate enough prediction of effective dielectric constants of composite to facile the research and development effort. Moreover, effective properties of composites, no matter whether they are dielectric or not, are of general theoretical and applied interest. For example, the properties of conductor-insulator composites were a subject for extensive experimental and theoretical investigations [4–7].

It is commonly believed that the effective properties of diphase composite are strongly dependent on the properties and the volume fraction of each phase, as well as particle shapes, spatial distribution, and their connectivity [8]. The shape parameters of the particle generally determine its depolarization and demagnetization factors, which are important parameters in some equations for the effective properties of composites [8]. In some fiber composites, where the minor phase particles may well disperse in matrix phase or distribute with some degrees of aggregation, it has been found that the degree of aggregation is the principal determinant of bulk conductivity of the composites, eclipsing the effects of orientation and fiber volume fraction [9].

*To whom all correspondence should be addressed. E-mail: wuyugong@yahoo.com.cn

The connectivity of the individual phases in composites controls the electric and magnetic flux patterns, as well as the mechanical stress and the transport properties [8]. The physical properties of composites can change by many orders of magnitude depending on the manner connections are made [8].

In addition to experimental and theoretical approaches, computer simulations have been adopted more and more frequently to study the effective properties of composites [10–12]. For example, Wakino et al. stimulated the effective dielectric constants of diphase dielectric composite using Monte Carlo-finite element method (MC-FEM) on a two-dimensional 25×25 matrix of small squares [12]. By observing the curve of effective dielectric constants calculated by MC-FEM, they proposed a modified form of the logarithmic rule and considered it as the most efficient predictive equation at that time [12]. We explored some new features of effective dielectric constants of diphase composite dielectrics in previous MC-FEM simulations on a 200×200 matrix of small squares and found that there actually existed equations that could give much better fit to the simulation data than modified logarithmic rule [13].

So far, simulations of dielectric properties of three-dimensional structures are very rare [14] and only those on periodic lattice were reported [15]. In this paper, we give the first MC-FEM simulation of effective dielectric constants of diphase composites on three-dimensional random structure. The dielectric constants of the two phases are taken as $\varepsilon_l = 1$ and $\varepsilon_h = 10$, 20, 50, 70, 100, 200, 300, 400, 500, 600, and 700; and $C = \varepsilon_h : \varepsilon_l$ is termed the dielectric constant contrast. (For systems with the same C values but $\varepsilon_l > 1$, one can multiply our simulation results with ε_l to obtain corresponding effective dielectric constants.) The volume fraction of each phase goes from 0.05 to 0.95. Several mixing rules and equations are then fitted to the simulated effective dielectric constants and the accuracy and relevance of the fits are thoroughly examined.

2. Theory

General Lichterecker mixing rule can be written as [16]

$$\varepsilon_m^\alpha = V_h \varepsilon_h^\alpha + V_l \varepsilon_l^\alpha \tag{1}$$

where ε_h and ε_l are the relative dielectric constants of the high-dielectric phase and low-dielectric phase, respectively, V_h and V_l the volume fractions of the high-dielectric phase and low-dielectric phase ($V_h + V_l = 1$), ε_m the effective dielectric constant of the composite, and α a parameter that determines the type of mixing rule.

When $\alpha = -1$, one has a serial mixing rule:

$$\frac{1}{\varepsilon_m} = \frac{V_h}{\varepsilon_h} + \frac{V_l}{\varepsilon_l} \tag{2}$$

and when $\alpha = 1$, a parallel mixing rule:

$$\varepsilon_m = V_h \varepsilon_h + V_l \varepsilon_l \tag{3}$$

In the case where $\alpha \to 0$, Lichterecker proposed an intermediate form between the serial and parallel form called logarithmic mixing rule:

$$\log \varepsilon_m = V_h \log \varepsilon_h + V_l \log \varepsilon_l \tag{4}$$

There is one parameter in general Lichterecker mixing rule and none in logarithmic mixing rule.

Serial and parallel mixing rules give lower and upper limits of the dielectric constant.

Composite media described by serial and parallel mixing rule are obviously highly anisotropic. Hashin and Shtrikman provided a tighter magnetic permeability bounds for macroscopically homogenous and isotropic composites [17]. Written in terms of dielectric constants, the Hashin-Shtrikman upper bound is

$$\varepsilon_m = \varepsilon_h + \frac{V_l}{\frac{1}{\varepsilon_l - \varepsilon_h} + \frac{V_h}{3\varepsilon_h}} \tag{5}$$

and the Hashin-Shtrikman lower bound is

$$\varepsilon_m = \varepsilon_l + \frac{V_h}{\frac{1}{\varepsilon_h - \varepsilon_l} + \frac{V_l}{3\varepsilon_l}} \tag{6}$$

The composite microstructures characterized by Hasshim-Shtrikman bounds are well described in [7, 18, 19].

Wakino et al. proposed a modified form of the logarithmic mixing rule [12]:

$$\varepsilon_m^{V_h - V_c} = V_h \varepsilon_h^{V_h - V_c} + V_l \varepsilon_l^{V_h - V_c} \tag{7}$$

where V_c was so-called critical volume fraction of the high-dielectric constant phase and it was at the point V_c that curves of ε_m simulated by MC-FEM on 2D lattice

and predicted by logarithmic mixing rule intersected each other [12].

Effective medium theory treats the dielectric response of a heterogeneous system by assuming that each particle is, on average, surrounded by a mixture that has the assumed homogeneous medium property (ε_{hm}) [20]. From the macroscopic polarization, the dielectric constant of a system with spherical particles can be written as

$$\varepsilon_m = \varepsilon_{hm}\left(1 + 2\sum_i V_i \frac{\varepsilon_i - \varepsilon_{hm}}{\varepsilon_i + 2\varepsilon_{hm}}\right) \times \left(1 - \sum_i V_i \frac{\varepsilon_i - \varepsilon_{hm}}{\varepsilon_i + 2\varepsilon_{hm}}\right)^{-1} \tag{8}$$

where $i = h$ or l. According to the self-consistent effective medium theory, ε_{hm} can be reasonably approximated as ε_m (i.e., $\varepsilon_{hm} = \varepsilon_m$), thus giving

$$V_h \frac{\varepsilon_h - \varepsilon_m}{\varepsilon_h + 2\varepsilon_m} + V_l \frac{\varepsilon_l - \varepsilon_m}{\varepsilon_l + 2\varepsilon_m} = 0 \tag{9}$$

This equation is usually known as the Bruggeman symmetrical medium equation. The microstructure of Bruggeman symmetrical medium is also described in [7, 18, 19].

Bruggeman symmetrical medium equation can be written in a more general form for oriented ellipsoids [21]:

$$V_h \frac{\varepsilon_h - \varepsilon_m}{\varepsilon_h + A\varepsilon_m} + V_l \frac{\varepsilon_l - \varepsilon_m}{\varepsilon_l + A\varepsilon_m} = 0 \tag{10}$$

Here A is a non-fixed parameter, which can be further written as

$$A = \frac{1 - V_c}{V_c} \tag{11}$$

where V_c is the critical volume fraction of the high-dielectric constant phase, and for spheres $V_c = \frac{1}{3}$. Because general Bruggeman symmetrical medium equation treats both phases on a completely symmetrical basis, it is expected that it is applicable to composite where both phases have similar morphologies and are distributed randomly through the whole system [2].

Percolation theory, whose objective is to characterize the connectivity properties in random geometries and to explore them with respect to physical processes, thus provides a natural frame for the theoretical description of random composites [22]. Percolation theory gives a phenomenological power-law dependence of the effective property of a diphase composite in the volume fraction range where one phase has just or is about to form a continuous percolation network or infinite cluster [2]. However, the main problem with using percolation theory in practical case is that it is only strictly valid when the ratio of the properties of the two phases is infinite or zero [23].

General effective media (GEM) equation, which combines most aspects of both percolation theories and effective media theories, can be written as [6]:

$$\frac{V_l\left(\varepsilon_l^{1/t} - \varepsilon_m^{1/t}\right)}{\varepsilon_l^{1/t} + A\varepsilon_m^{1/t}} + \frac{V_h\left(\varepsilon_h^{1/t} - \varepsilon_m^{1/t}\right)}{\varepsilon_h^{1/t} + A\varepsilon_m^{1/t}} = 0 \tag{12}$$

Here, A is also related to V_c by Eq. (11), and t is an exponent parameter. GEM equation reduces to various other theoretical expressions, with specified combinations of A and t [8]. It has been shown that GEM equation was both an effective media interpolation formula and a matched asymptotic expression for percolation equation [8].

The modified form of GEM equation can be written as [4, 5]:

$$\frac{V_l\left(\varepsilon_l^{1/s} - \varepsilon_m^{1/s}\right)}{\varepsilon_l^{1/s} + A\varepsilon_m^{1/s}} + \frac{V_h\left(\varepsilon_h^{1/t} - \varepsilon_m^{1/t}\right)}{\varepsilon_h^{1/t} + A\varepsilon_m^{1/t}} = 0 \tag{13}$$

where s is another exponent term as t, and A is also related to V_c by Eq. (11). GEM equation and modified GEM equation were extensively used to fit ac and dc conductivity and complex dielectric constant of composites [4–8].

3. Algorithm

3.1. MC-FEM

Our simulations are performed using the Monte Carlo-finite element method (MC-FEM). The cubic space is first divided into $N \times N \times N$ cubic subcells, each of which can be designated as either low-dielectric constant phase (ε_l) or high-dielectric constant phase (ε_h) [Fig. 1(a)]. The electrical potential difference between the parallel electrodes is $U_0 = 10\,V$. According to the volume fraction of high-dielectric constant phase

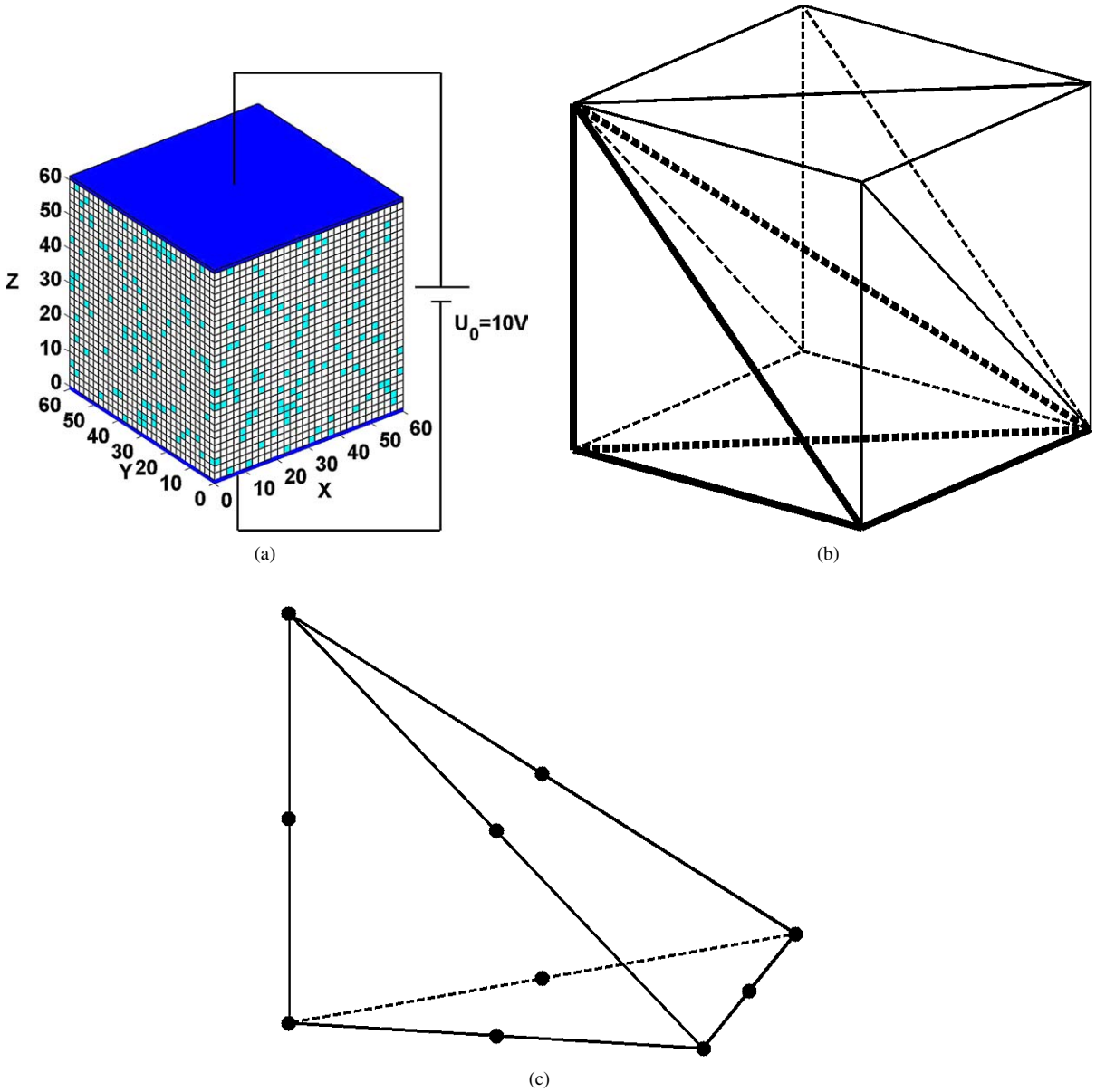

Fig. 1. (a) The cubic lattice is first divided into $N \times N \times N$ subcells ($30 \times 30 \times 30$ in this illustration) and each subcell is assigned to high-dielectric constant phase (the gray one) or low-dielectric constant phase (the white one) using random number generator according to V_h (15% in this illustration). (b) Every subcell is then subdivided into 6 tetrahedronal finite elements (the bold lines show one of them). (c) On each tetrahedronal finite element, 10 points (4 vertexes and 6 midpoints) are chosen as nodes.

($V_h = 0.05$–0.95), the property of each cubic subcell (ε_h or ε_l) is determined by standard Monte Carlo method using random number generator. Each subcell is divided further into 6 tetrahedronal finite elements [Fig. 1(b)], on each of which 10 points (4 vertexes and 6 midpoints of edges) are chosen as nodes [Fig. 1(c)]. Within a tetrahedronal element, it is assumed that the potential is approximated by the expression [24]:

$$u = C_1 + C_2x + C_3y + C_4z + C_5x^2 + C_6y^2 + C_7z^2 + C_8xy + C_9yz + C_{10}zx \tag{14}$$

where x, y, and z are coordination of point and C_i ($i = 1$–10) are coefficients. The energy associated with a single cubic element is determined by the following equation:

$$w_i = \frac{1}{2}\varepsilon_0 \int_v \varepsilon_i (\nabla u)^2 dv \tag{15}$$

where ε_i is either ε_h or ε_l and ε_0 is the permittivity of vacuum. The total energy associated with an assemblage of all elements is the sum of all the element energies and can be written as

$$W = \frac{1}{2} U^T S U \tag{16}$$

where U is a column vector, which indicates potential of each node and S a matrix. According to the theory [24], configuration of the electrical field gives a minimum energy, i.e.,

$$\frac{\partial W}{\partial u_r} = 0 \tag{17}$$

where u_r is the rth element of U. Equation (17) yields a linear equation system

$$DU = b \tag{18}$$

where D is a sparse matrix and b a column vector. This linear equation system is resolved and the energy of the system can then be calculated. According to the relation

$$W = \frac{1}{2}\varepsilon_0 \varepsilon_m E^2 \tag{19}$$

where E is the voltage between electrodes, the effective dielectric constant is obtained out eventually. The FEM algorithm in this section is based on reference [24].

3.2. *Accuracy of the Effective Dielectric Constants*

One of the basic principles underlying MC-FEM algorithm is the search of the lowest energy of the system. If the resolution of Eq. (18) were not precise enough, the energy of the system and therefore the effective dielectric constant calculated would be incorrectly greater. To estimate the accuracy of our algorithm, FEM calculations are performed on serial mixing system with adjacent layers of different phases for various Ns and Cs. At each fixed N and C, the effective dielectric constant of the system can be calculated theoretically using serial mixing rule, and the electrical potential of each node can also be calculated exactly. The differences between potentials obtained using Eq. (18) and the theoretical ones are recorded for all nodes, and the greatest difference, μ, is regarded as the potential precision of this FEM calculation. It has been found that when C and V_h are fixed, μ increases monotonously as N rises and that when N and V_h are fixed, μ increases monotonously as C rises. When $N = 30$ and $C = 700$ (the most rigorous conditions in present work, since these are the maximum N and C), our algorithm can guarantee a μ value equal to or less than 1×10^{-10} v for serial mixing system, and the difference between effective dielectric constant calculated by FEM and the theoretical one is less than 1.54×10^{-7}, accurate enough for the purpose of this work.

3.3. *Coefficients of Variation*

This paper uses subcells whose property (ε_h or ε_l) is randomly assigned according to volume fraction of each phase to simulate the distributions of grains of the two phases in composites. Therefore a series of ε_ms computed with the same V_h and C show some degree of fluctuation, an inevitable nature of Monte Carlo simulation. Such fluctuation can be measured by coefficients of variation of data (CV, standard deviation divided by average) (Fig. 2). In this paper, for each combination of C, V_h, and N, a group of $\varepsilon_{m,i}$ are computed on different microstructure ($i = 1, \ldots, 20$) to obtain their standard deviations, average values, and CV. It has been noticed that when other conditions are fixed, CV decreases obviously with the increase of N [Fig. 2(a)], and nearly always increases with the augment of C. Moreover, at given C and N, CV is relatively greater when V_h is between 0.1 and 0.2, and CV reaches its maximum when V_h is in the vicinity of 0.15 [Fig. 2(b)]. In this paper, N is chosen to be 30 when $V_h = 0.1$, 0.15 and $C = 300$–700, and 20 in other conditions. As a result, all CV values of ε_ms calculated in this paper are less than 5.5% [Fig. 2(b)].

3.4. *Parameter Fitting*

In this paper, with each C fixed, a serial of 19 ε_ms ($V_h = 0.05$–0.95) are obtained. Thereafter, various

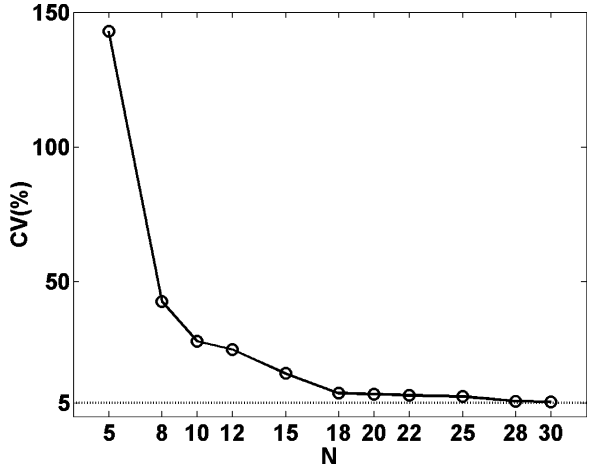

(a)

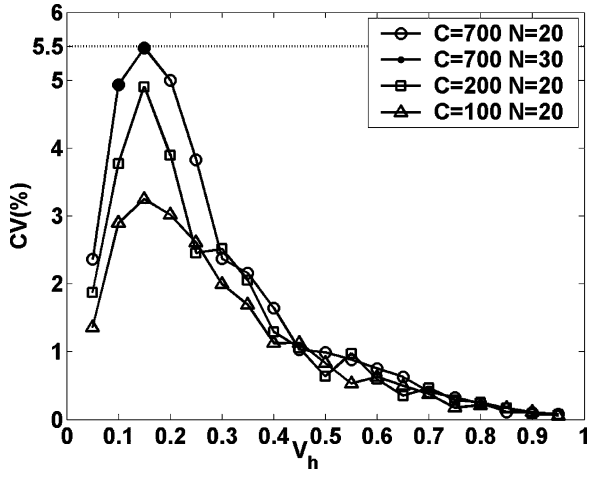

(b)

Fig. 2. (a) When $C = 700$, $V_h = 0.15$, coefficients of variation (CV) as a function of N. (b) When $C = 100$, 200, and 700, coefficients of variation (CV) as a function of V_h.

mixing rules and equations are fitted to ε_ms simulated by varying the non-fixed parameters to minimize the quantity [6]

$$\chi = \left[\frac{1}{n-p} \sum_{i=1}^{n} \left(\frac{\varepsilon_m - \varepsilon_{equ}}{0.01\varepsilon_m} \right)^2 \right]^{\frac{1}{2}} \tag{20}$$

Here ε_{equ} is the effective dielectric constant calculated by equations using the appropriate variable parameters, n is the number of data points and p is the number of variable parameters of each function. If $\chi = 1$, it is claimed that data have been fitted to an accuracy of 1% in this case of specified C.

The algorithm for minimizing χ is based on the solution of corresponding Kuhn-Tucker equation through sequential quadratic method [25].

4. Results and Discussion

4.1. Effective Dielectric Constants

In Figs. 3(a) and (b), the effective dielectric constants simulated using MC-FEM are given (when $V_h = 0$ or 1, ε_m is ε_l or ε_h, respectively). Thereafter, for each plot of ε_m vs. V_h, we introduce a quantity $R = \frac{\varepsilon_m(V_h) - \varepsilon_m(V_h - 0.05)}{\varepsilon_m(V_h)}$, where $V_h = 0.05$–1, to indicate the relative increasing rate of ε_m between V_h-0.05 and V_h (Fig. 4). Two features are evident: First, all curves of R vs. V_h peak at the point of $V_h = 0.15$, which means that for each C, ε_m increases relatively most rapidly as V_h rises from 0.1 to 0.15. Second, when V_h is 0.15, R increases monotonously with the augment of C, which means that larger C value leads to greater relative increasing rate of ε_m.

In Figs. 5(a)–(c), we show the potential contours on section planes vertical to X, Y, and Z axes, when $C = 700$ and $V_h = 0.15$. The high-dielectric phase subcells sectioned by these planes are also marked. It is evident that potential contours on these sections all tend to distribute in such a manner as to avoid passing through high-dielectric phases. This behavior was also observed on 2D lattice simulation [12, 13].

4.2. Mixing Rules Fitting

The parameters of general Lichterecker mixing rule for each C are plotted in Fig. 6(a). Parameter α decreases monotonously from 0.44 to 0.33 with the augment of C. It can be observed from Fig. 6(b) that when $C = 20$ Lichterecker mixing rule can well fit the simulation results. For all C values, the curves of ε_m calculated by logarithmic mixing rule never intersect the curves of simulated ε_m (except when $V_h = 0$ or 1), as shown in Figs. 6(b) and (c). Chen measured the effective dielectric constants of PMN-pyrochlore system at 25°C, where the dielectric constants of PMN and pyrochlore were 14138 and 153.3, respectively [2]. He also noticed that the curve of experimental ε_m did not intersect with the curve of ε_m predicted by logarithmic mixing rule [2]. However, this was not the case in 2D simulations, where these two curves have one intersection [12, 13].

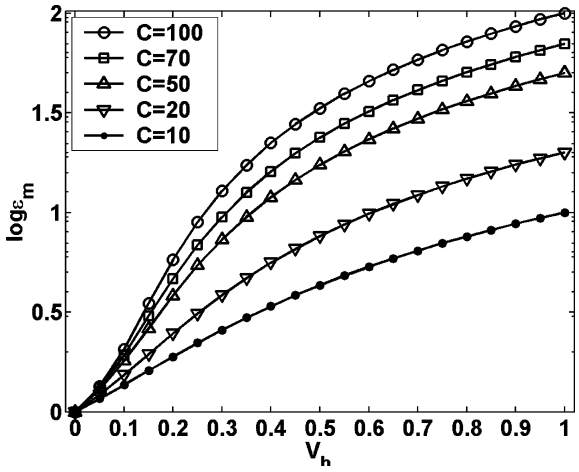

(a)

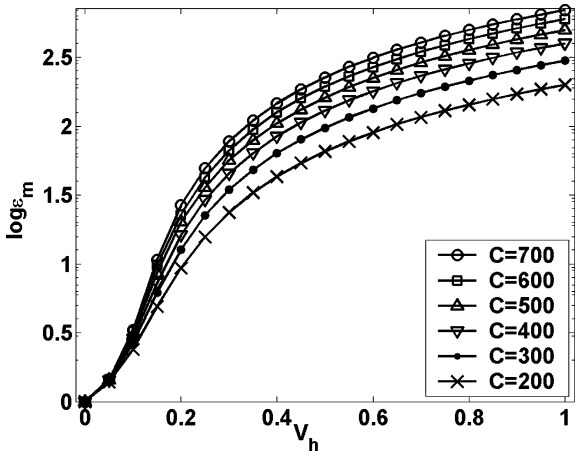

(b)

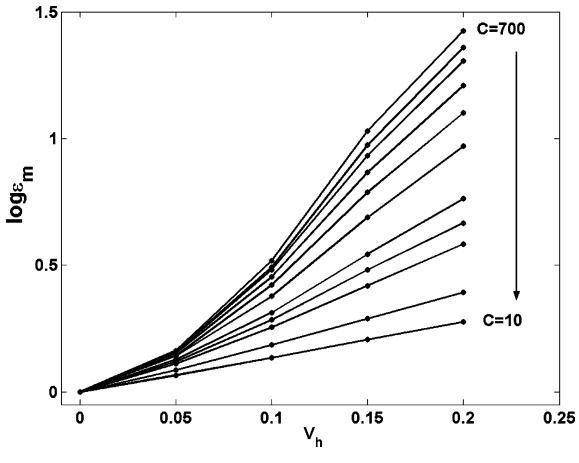

(c)

Fig. 3. (a) ε_m simulated for $C = 10, 20, 50, 70$, and 100. (b) ε_m simulated for $C = 200, 300, 400, 500, 600$, and 700. (c) ε_m simulated for all C values with V_h from 0 to 0.2.

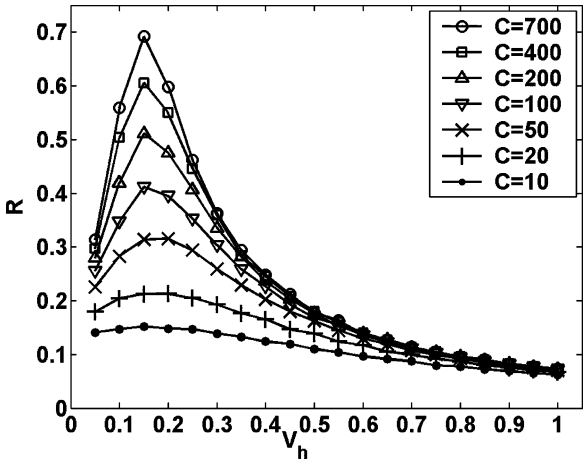

Fig. 4. Relative increasing rate (R) of ε_m, when $C = 10, 20, 50, 70, 100, 200, 400$, and 700.

Moreover, it is evident from Figs. 6(b) and (c) that the discrepancy between ε_m calculated by logarithmic mixing rule and simulated by MC-FEM is comparatively very large except when V_h is very high or very low. Therefore, one should be very cautious to use logarithmic mixing rule to predict effective dielectric constants of real dielectric materials.

Because there is no intersection between ε_m curves simulated on 3D system and calculated using logarithmic mixing rule, modified logarithmic mixing rule loses its physical basis, for its parameter V_c has become meaningless on 3D system.

When general Bruggeman symmetrical medium equation is fitted to ε_m simulated [Fig. 7(a)], it is evident that parameter A obtained for each C is larger than 2, and that as C rises, A increases monotonously from 2.91 to 4.39 [Fig. 7(b)].

Curves of parameter A in GEM equation and modified GEM equation are also plotted in Fig. 7(b). Both curves have a similar shape as that of A in general Bruggeman symmetrical medium equation. At the same C, modified GEM equation gives the greatest A and general Bruggeman symmetrical medium equation the smallest.

The critical volume fractions of the high-dielectric constant phase of general Bruggeman symmetrical medium equation, GEM equation, and modified GEM equation are also plotted as V_c vs. C in Fig. 7(c). In conductor-insulator composite media, the critical volume fraction for the high-conductivity phase typically varies between 0.01 and 0.6 [8]. A "basic" value of

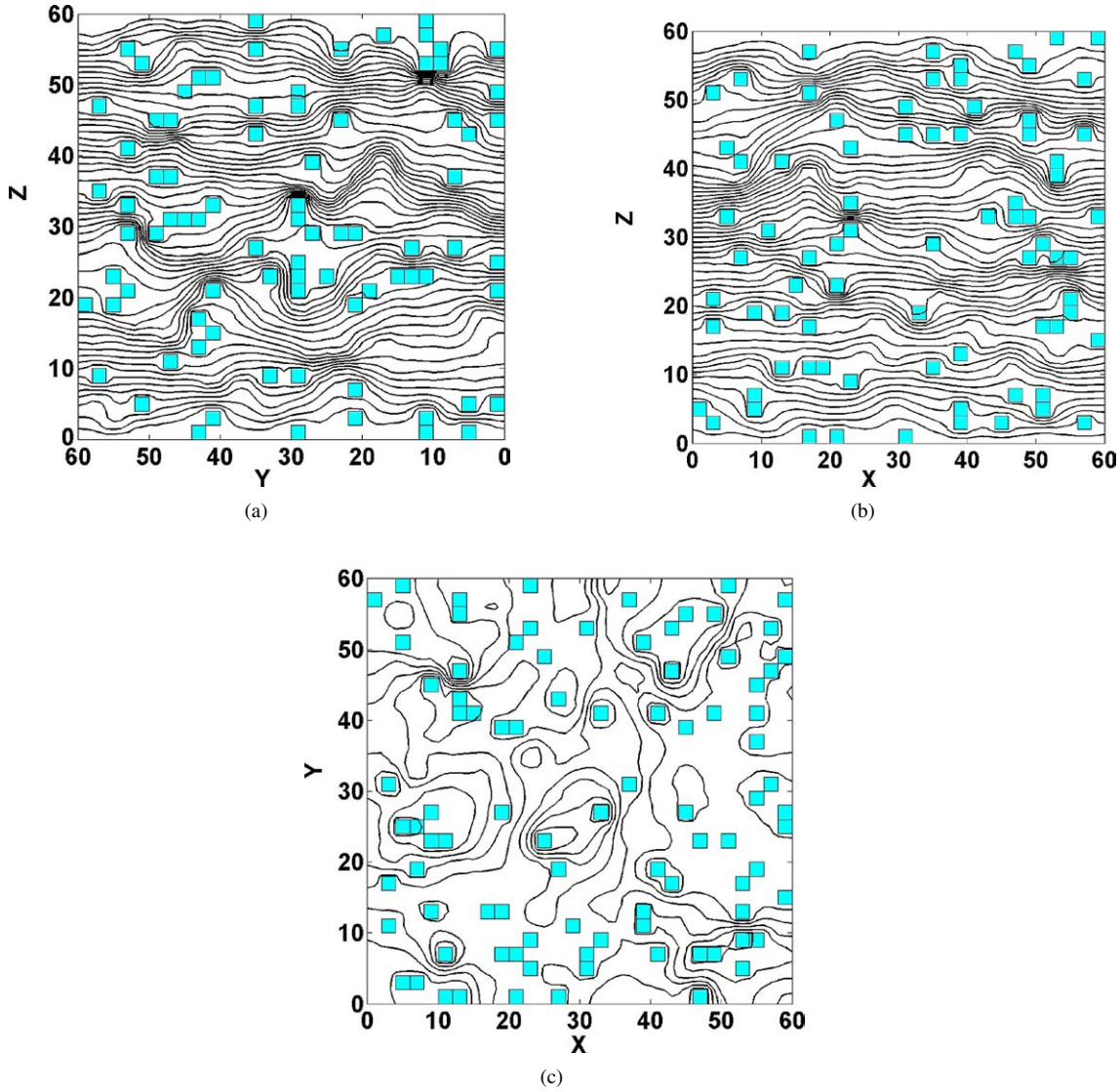

Fig. 5. When $C = 700$ and $V_h = 0.15$, potential contours on section planes: (a) $X = 15$, (b) $Y = 15$ and (c) $Z = 15$. The high-dielectric phases subcells are marked gray.

the critical volume fraction has been considered to be about 0.16 for conductor-insulator media, because this value is obtained whenever contacting conducting hard spheres are placed at random on a regular lattice or conducting hard spheres are randomly packed with equally, or near equally, sized insulating spheres [8]. It can be observed that when $C > 200$, V_c's obtained from fitting GEM equation are also around 0.16.

GEM equation and modified GEM equation can be best fitted to the simulated data [Fig. 8(a)]. Parameters t and s in modified GEM equation and t in GEM equation are shown in Fig. 8(b). As C rises from 10 to 700, t in GEM equation increases from 1.18 to 1.30; t in modified GEM equation from 1.19 to 1.37 monotonously. At the same C, the t value in modified GEM equation is slightly greater than that in GEM equation. The other parameter s in modified GEM equation decreases slightly yet steadily from 0.98 to 0.95 with the augment of C. Up until nearly fifteen years ago, it was widely believed that exponents s and t should be universal and

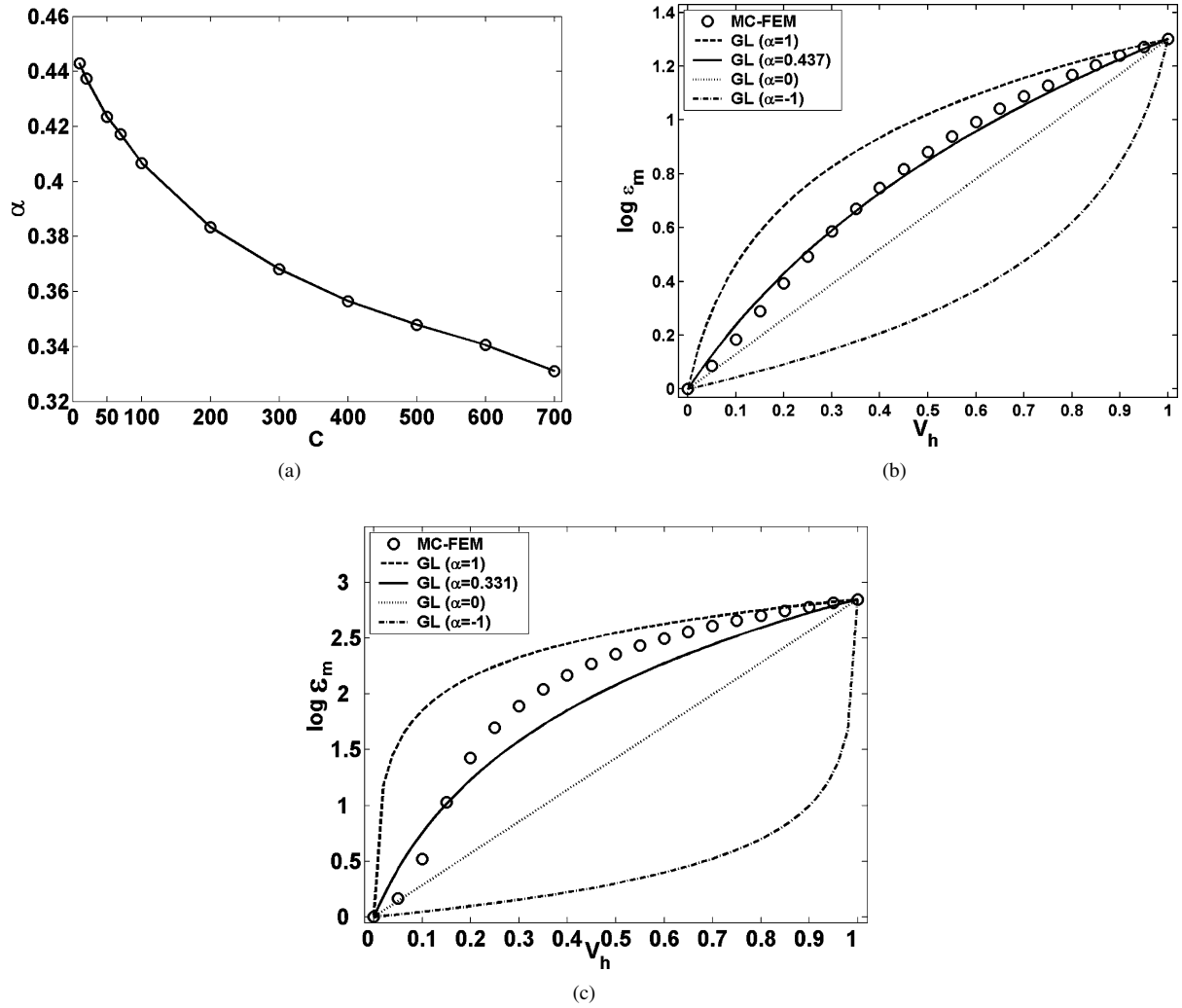

Fig. 6. General Lichterecker mixing rule (GL) fitted to ε_m simulated: (a) Parameter α in general Lichterecker mixing rule (GL). (b) When $C = 20$, ε_m simulated by MC-FEM and calculated by general Lichterecker mixing rule (GL) with $\alpha = 1, 0.437, 0$, and -1. (c) When $C = 700$, ε_m simulated by MC-FEM and calculated by general Lichterecker mixing rule (GL) with $\alpha = 1, 0.331, 0$, and -1.

depend on the dimensions of the system only. The most widely accepted universal values, in three dimensions, were $s \approx 0.87$and $t \approx 2.0$ [26], and in some work values of t in the range of 1.7 to 2.0 were also considered acceptable. Since then a number of continuum systems in which unequivocal nonuniversal exponents have been observed or predicted [4, 5, 7, 8]. For instance in systems where various conducting powders were distributed on large insulating grains, values of s in the range 0.35–1.3 and t in the range 1.7–5.8 were observed [27]. In conductor-insulator composites, the contrast of properties of the two phases, i.e., ratio of conductivities, is usually greater than 10^8, while the maximum dielectric constant contrast in our simulation is only 700. It seems that the lower dielectric constant contrasts may, at least partially, attribute to the lower t values in present work.

4.3. Evaluation of Mixing Rules

From Fig. 9, it can be observed that when $V_h > 0.8$, ε_m simulated is very approximate to the upper limit predicted by Hashin-Shtrikman upper bound and when

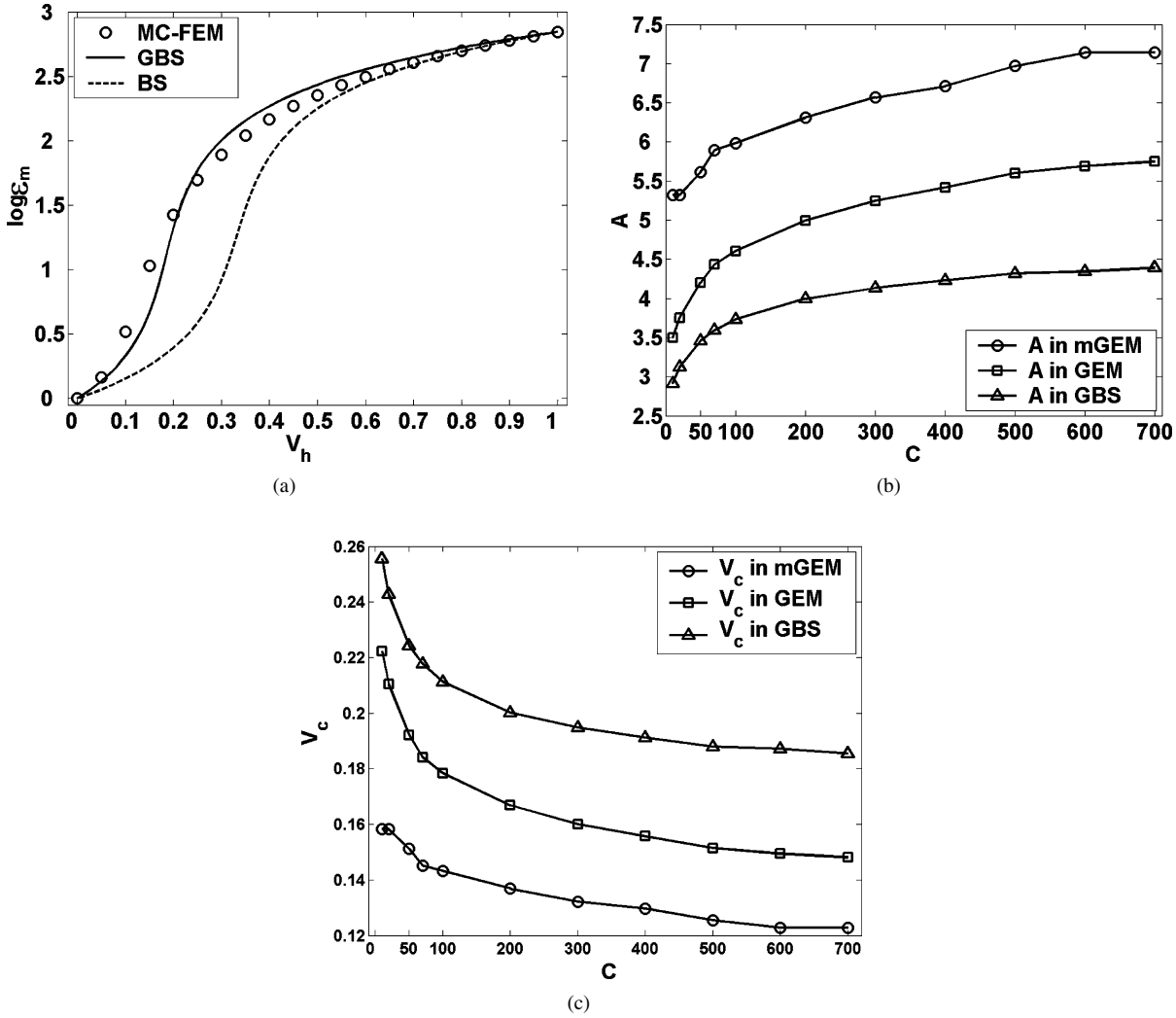

Fig. 7. General Bruggeman symmetrical medium equation (GBS) and Bruggeman symmetrical medium equation (BS) fitted to ε_m simulated: (a) When $C = 700$, ε_m simulated by MC-FEM and calculated by general Bruggeman symmetrical medium equation (GBS) with $A = 4.39$, and Bruggeman symmetrical medium equation (BS). (b) Parameter A in general Bruggeman symmetrical medium equation (GBS), GEM equation (GEM), and modified GEM equation (mGEM). (c) Parameter V_c in general Bruggeman symmetrical medium equation (GBS), GEM equation (GEM), and modified GEM equation (mGEM).

$V_h = 0.95$, it even exceeds this bound. It has been found that when $V_h = 0.95$ for all C values and when $V_h = 0.9$ for $C = 10$, ε_ms simulated are a little higher than Hashin-Shtrikman upper bound. The largest deviation is 0.11% at $V_h = 0.95$ and $C = 20$. Hashin-Shtrikman bounds were derived theoretically and supposed to be applicable to macroscopically homogenous and isotropic media [17]. Actually, they were attained in special Hashin-Shtrikman microgeometry [7, 17–19]: the composite is made up entirely of multicoated ellipsoids, in which all the interfaces are confocal ellipsoidal surfaces. The ellipsoids must come in all sizes in order to fill up entire volume, but they must all have the same ratios of axes, as well as the same arrangement and volume fractions of the various components, and they must all be similarly oriented [7, 17–19]. One possible reason for the bound breaking behavior in present work is that our models with limited number of equally-sized subcells ($20\times20\times20$) may not be macroscopically isotropic and homogenous in the sense of Hashin-Shtrikman microgeometry. Moreover, similar bound breaking behavior [18] was also noticed

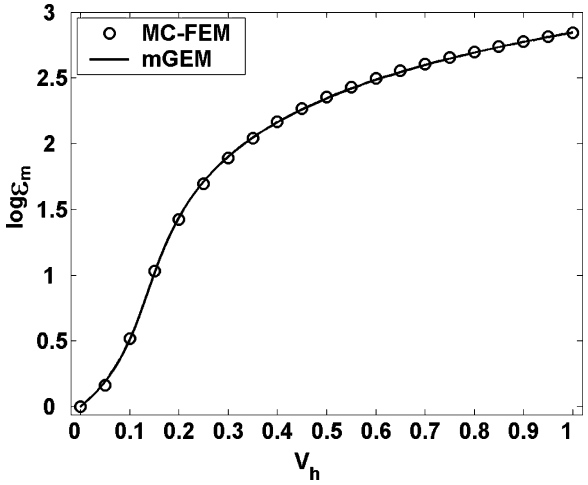

(a)

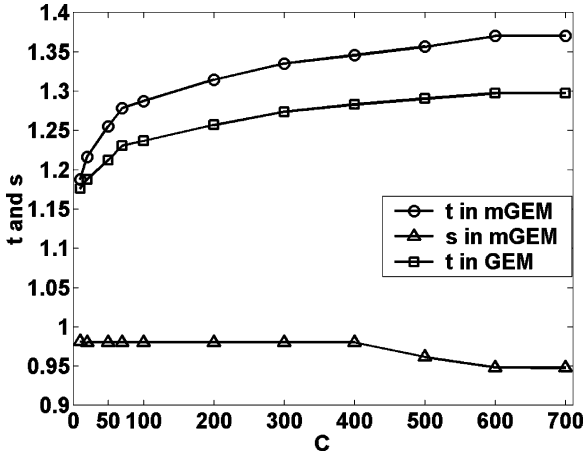

(b)

Fig. 8. GEM equation (GEM) and modified GEM equation (mGEM) fitted to ε_m simulated: (a) When $C = 700$, ε_m simulated by MC-FEM and calculated by modified GEM equation (mGEM) with $A = 7.14$, $t = 1.37$, and $s = 0.95$. (b) Parameters t and s in modified GEM equation (mGEM), and t in GEM equation (GEM). The plots of ε_m calculated using GEM equation do not appear in Fig. 8(a) for the distinctness of curves, because of the similarity between ε_m's calculated by GEM equation and modified GEM equation.

for the conductivity of cubic bricklayer model [28], which also has cubic structures. We also note that when $V_h > 0.6$, the curve of general Bruggeman symmetrical medium equation also lies outside Hashin-Shtrikman upper bound (Fig. 9). This is because general Bruggeman symmetrical medium equation (except for $A = 2$) is for oriented ellipsoids, which gives an anisotropic media.

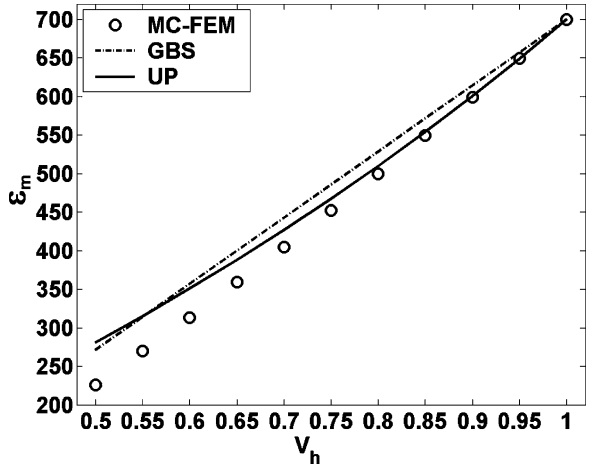

Fig. 9. When $C = 700$, comparison between ε_m simulated by MC-FEM, and calculated by Hashin-Shtrikman up bound (UP) and General Bruggeman symmetrical medium equation (GBS) with $A = 4.39$.

Although logarithmic mixing rule is extensively used to fit data, its representation of ε_m simulated by MC-FEM is unsatisfactory [Fig. 10(a)]. The χ of general Lichterecker mixing rule is lower than that of logarithmic mixing rule for each C value, but higher than that of general Bruggeman symmetrical medium equation. When $C > 70$, χ's of general Bruggeman symmetrical medium equation increases rapidly with the augment of C [Fig. 10(b)]. The χ values of GEM equation and modified GEM equation also increase with C rising, but much more slowly, and their maximum is less than 4. Considering that ε_m simulated by MC-FEM has the greatest CV value of 5.5%, two conclusions may be drawn: (1) GEM equation and modified GEM equation can be used to fit ε_m simulated most accurately. (2) In the whole range of volume fraction, GEM equation gives a fit to the data as statistically good or nearly as good as that using modified GEM equation. Similar conclusions were also suggested by Wu and McLachlan when fitting GEM equation and modified GEM to conductivity of composite media [5]. Therefore, in the research and development of composite dielectrics, it is advisable to choose either GEM equation or modified GEM equation as predictive equation.

4.4. Comparison with Experimental Data

Dielectric constants of PMN-pyrochlore and TiO_2-ZrO_2 composites are given in Figs. 11 and 12,

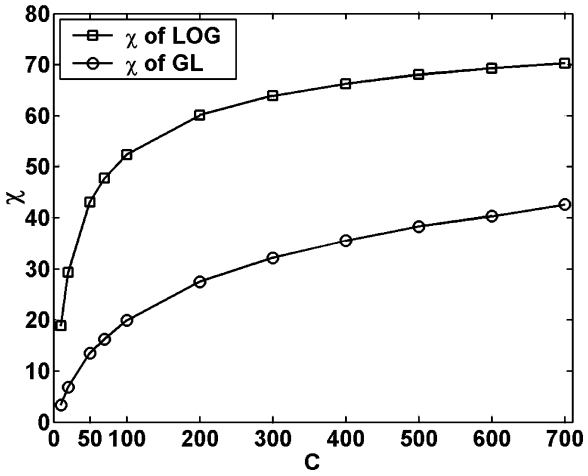

(a)

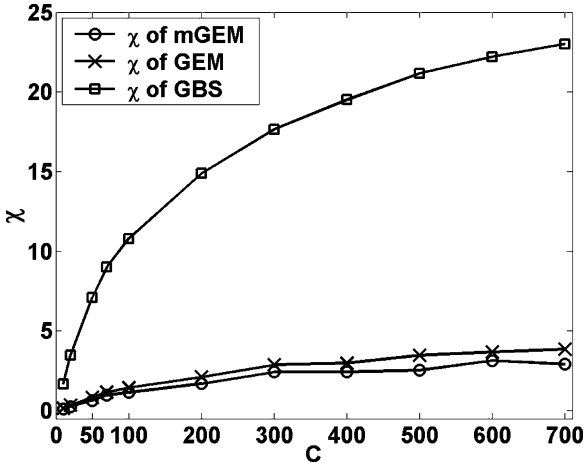

(b)

Fig. 10. (a) Fitness checks of logarithmic mixing rule (LOG) and general Lichterecker mixing rule (GL). (b) Fitness checks of general Bruggeman symmetrical medium equation (GBS), GEM equation (GEM) and modified GEM equation (mGEM).

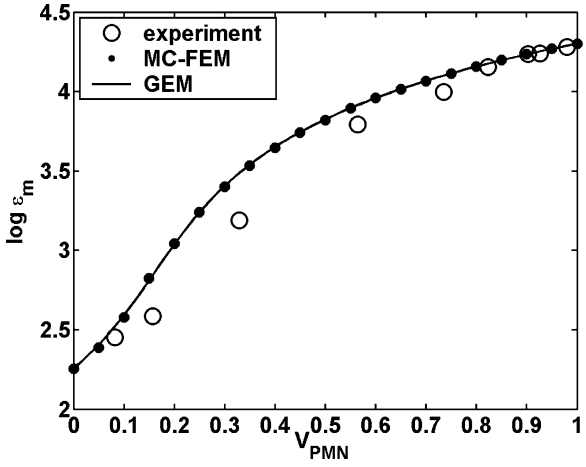

(a)

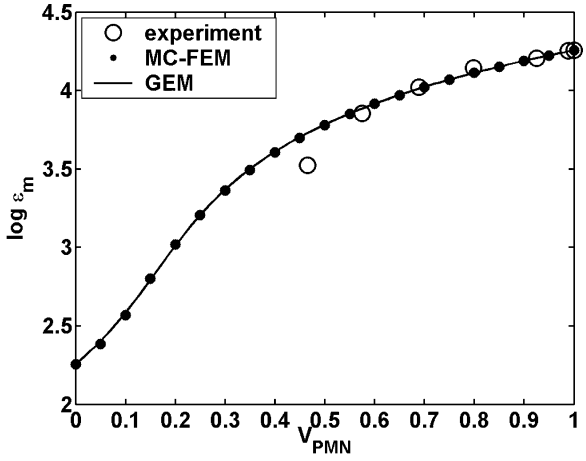

(b)

Fig. 11. Dielectric constants of PMN-pyrochlore composites: (a) experimental data in [29], MC-FEM simulation results, and the predictions of GEM equation (GEM) with $A = 4.66$ and $t = 1.24$. (b) experimental data in [30], MC-FEM simulation results, and the predictions of GEM equation (GEM) with $A = 4.61$ and $t = 1.24$.

respectively; both experimental data [29–31] and simulation results are shown. It is evident that our simulation results are in good agreement with most of the experimental data. Especially when the volume fraction of high dielectric phase in composites is higher than 0.6, MC-FEM simulation can represent the dielectric constants of PMN-pyrochlore and TiO_2-ZrO_2 composites very well. GEM equation is also fitted to the simulation results and corresponding parameters obtained.

5. Conclusion

Effective dielectric constants of diphase composite dielectrics are simulated by Monte Carlo-finite element method on a cubic lattice in three dimensions. The ratio of the dielectric constants of the two phases goes from 10 to 700. Several mixing rules and equations are fitted to the simulation results and the accuracy and relevance of the fits are thoroughly examined. Parameters obtained through fitting general Lichterecker mixing rule, general Bruggeman symmetrical medium

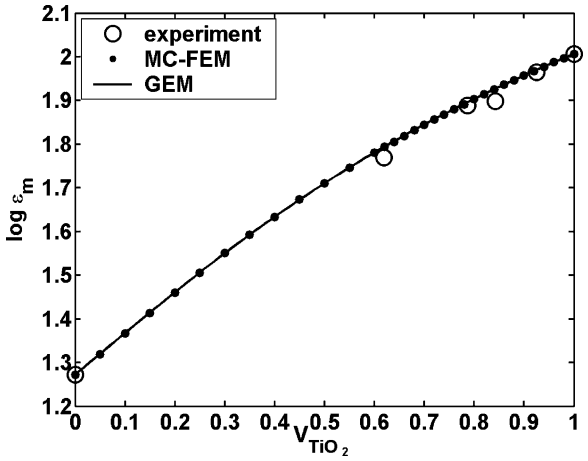

Fig. 12. Dielectric constants of TiO_2-ZrO_2 composites: (a) experimental data in [31], MC-FEM simulation results, and the predictions of GEM equation (GEM) with $A = 3.40$ and $t = 1.20$.

equation, GEM equation and modified GEM equation are given for each ratio of the dielectric constants of the two phases. These parameters are all found to increase or decrease monotonously as the ratio of the dielectric constants of the two phases rises. Modified logarithmic mixing rule loses its physical basis when fitted to three-dimensional data. GEM equation and modified GEM equation give the best fits to the dielectric constants simulated and the accuracy of their fits is comparable. The dielectric constants simulated for composite systems, such as PMN-pyrochlore and TiO_2-ZrO_2, are in good agreement with the experimental data. The simulation results are therefore applicable for the prediction of the dielectric constants of these composite systems.

References

1. T.R. Shrout and A. Halliyal, *Am. Ceram. Soc. Bull.*, **66**, 704 (1987).
2. J. Chen, Microstructure-Property Relations in the Complex Perovskite Lead Magnesium Niobate, Ph.D. Thesis, Leigh University, Pennsylvania State, USA (1991).
3. A. Nakano, D.P. Cann, and T.R. Shrout, *Jpn. J. Appl. Phys. A*, **36**, 1136 (1997).
4. J. Wu and D.S. McLachlan, *Phys. Rev. B*, **56**, 1236 (1997).
5. J. Wu and D.S. McLachlan, *Phys. Rev. B*, **58**, 14880 (1998).
6. D.S. McLachlan, *J. Phys. C: Solid State Phys.*, **20**, 865 (1987).
7. D.J. Bergman and D. Strout, in *Solid State Physics*, edited by H. Ehrenreich and D. Turnbull (Academic, San Diego, 1992), p. 147.
8. D.S. McLanchlan, M. Blaszkiewicz, and R. E. Newnham, *J. Am. Ceram. Soc.*, **73**, 2187 (1990).
9. P.C. Sturman and R.L. McCullough, *J. Appl. Phys.*, **72**, 2883 (1992).
10. H.E. Roman, A. Bunde, and W. Dieterich, *Phys. Rev. B.*, **34**, 3439 (1986).
11. M. Bartkowiak, G.D. Mahan, F.A. Modine et al., *J. Appl. Phys.*, **80**, 6516 (1996).
12. K. Wakino, T. Okada, N. Yoshida et al., *J. Am. Ceram. Soc.*, **76**, 2588 (1993).
13. X. Zhao and Y. Wu, *J. Mater. Sci.*, **39**, 291 (2004).
14. E. Tuncer, Y.V. Serdyuk, and S.M. Gubanski, *IEEE Transactions on Dielectrics and Electrical Insulation*, **9**, 809 (2002).
15. B. Sareni, L. Krahenbuhl, and A. Beroual, *J. Appl. Phys.*, **80**, 1688 (1996).
16. K. Lichtenecker, *Phys. Z.*, **27**, 115 (1926).
17. Z. Hashin and S. Shtrikman, *J. Appl. Phys.*, **33**, 3125 (1962).
18. D.S. McLanchlan, J.H. Hwang, and T.O. Mason, *Journal of Electroceramics*, **5**, 37 (2000).
19. D.S. McLanchlan, *Journal of Electroceramics*, **5**, 93 (2000).
20. I. Webman, J. Jortner, and M.H. Cohen, *Phys. Rev. B*, **15**, 5712 (1977).
21. F. Brouers, *J. Phys. C: Solid State Phys.*, **19**, 7183 (1987).
22. A. Bunde and W. Dieterich, *Journal of Electroceramics*, **5**, 81 (2000).
23. D.S. McLachlan and J. Chen, *J. Phys.: Condens. Matter*, **4**, 4557 (1992).
24. J. Jin, *The Finite Element Method in Electromagnetics* (John Wiley & Sons, Inc., New York, 1993), p. 256.
25. Y. Yuan, *Numerical Method For Nonlinear Programming* (Shanghai Scientific & Technical Publishers, Shanghai, 1993), p. 207.
26. D.S. Stauffer and A. Aharony, *Introduction to Percolation Theory* (Taylor and Francis, London, 1994).
27. C. Chiteme and D.S. McLachlan, *Phys. Rev. B*, **67**, 024206 (2003).
28. J.H. Hwang, D.S. McLanchlan, and T.O. Mason, *Journal of Electroceramics*, **3**, 7 (1999).
29. J. Chen and M.P. Harmer, *J. Amer. Ceram. Soc.*, **73**, 68 (1990)
30. K. Huh, J. Kim, and S. Cho, in *Proc. of Fulrath Memorial Int'l Symp. on Advanced Cera.*, edited by N. Ichinose (CNT Inc., Tokyo, 1993), p. 61.
31. W.D. Kingery, *Introduction to Ceramics* (Wiley, New York, 1976).